JPE 16-4-15

http://dx.doi.org/10.6113/JPE.2016.16.4.1387
ISSN(Print): 1598-2092 / ISSN(Online): 2093-4718

A Simple Method for Identifying Mechanical Parameters Based on Integral Calculation

Sang-Heon Han*, Anno Yoo**, Sang Won Yoon***, and Young-Doo Yoon†

*,†Dept. of Electrical Eng., Myongji University, Yongin, Korea
**General Motors, Pontiac, MI, United States
***Dept. of Automotive Eng., Hanyang University, Seoul, Korea

Abstract

A method for the identification of mechanical parameters based on integral calculation is presented. Both the moment of inertia and the friction constant are identified by the method developed here, which is based on well-known mechanical differential equations. The mechanical system under test is excited according to a pre-determined low-frequency sinusoidal motion, minimizing the distortion, and increasing the accuracy of the results. The parameters are identified using integral calculation, increasing the robustness of the results against measurement noise. Experimental data are supported by simulation, confirming the effectiveness of the proposed technique. The performance improvements shown here are of use in the design of speed and position controllers and observers. Owing to its simplicity, this method can be readily applied to commercial inverter products.

Key words: Integral calculation, Mechanical parameter identification, Moment of inertia, off-line identification, Viscous friction coefficient

I. INTRODUCTION

Semiconductor and LCD panel manufacturing equipment, machine tools, and welding robots require precise, dynamic control to achieve high productivity and manufacturing accuracy [1], [2]. Industrial servo systems require rapid acceleration and deceleration to increase productivity through the reduction of mechanical settling times. Additionally, servo systems are influenced by mechanical parameter uncertainty and external disturbances. Rejection techniques are adopted to achieve a specified manufacturing accuracy. Therefore, highly dynamic motion controllers and disturbance observers are generally implemented in servo systems.

Many motion-control solutions consist of a motion controller and a torque controller in a cascaded control loop. The primary role of the torque controller is to generate a precise torque, with respect to a reference. The inner loop performance is critical. Therefore, various techniques have been studied including field oriented control (FOC) [3], direct torque control (DTC) [4]-[6] and predictive control [7], [8]. Using these techniques, a precise, stable actuator torque can be implemented.

If the torque control system is assumed to be ideal, the servo performance depends on the motion controller, which includes the feedback control, torque feedforward control [1], [2], anti-windup control [9] and disturbance observation [10]-[13]. In many servo applications, the mechanical systems to be controlled and their design parameters are known, but the mechanical parameters are inaccurate. When the economic requirements for the productivity and accuracy of manufacturing systems become more rigorous, precise mechanical parameters are essential. Therefore, to properly design these controllers, accurate identification of the mechanical parameters such as the moment of inertia and viscous friction coefficient is necessary.

Many papers have been presented on the subject of mechanical parameter identification by applying observer and adaptive control theory. Algorithms based on observer theory [14], [15] used a modified Luenberger observer to estimate inertia information based on state variables such as the speed and disturbance torque. Identification algorithm performance

Manuscript received Jul. 22, 2015; accepted Apr. 4, 2016
Recommended for publication by Associate Editor Gaolin Wang.
†Corresponding Author: ydyoon@mju.ac.kr
Tel: +82-31-330-6833, Myongji University
*Dept. of Electrical Eng., Myongji University, Korea
**General Motors, United States
***Dept. of Automotive Eng., Hanyang University, Korea

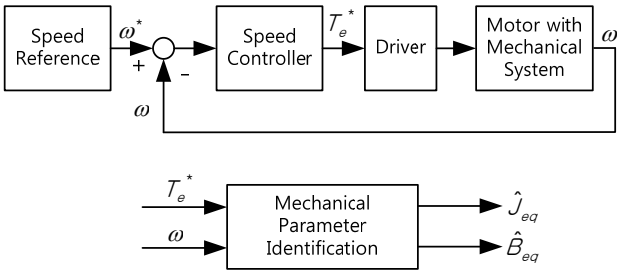

Fig. 1. Block diagram of mechanical parameter identification.

depends on the initial values, and an algorithm can fail if it is inappropriately initialized. Algorithms based on adaptive control theory [16]-[18] modify the modeled plant inertia values so that the plant model's estimated speed becomes the same as the actual speed. Implementation of these methods is complex, and the results are severely affected by adaptation gains.

In addition to the above approaches, off-line detection methods [19]-[22] have been proposed to avoid these problems. These techniques use variables such as speed, torque, and position to calculate the mechanical parameters from dynamic system equations. However, these algorithms need a pre-determined motion or speed profile, and can only determine the parameters off-line. Reference [19] utilized a triangular speed profile. As a result, the torque signal showed rectangular waveforms. Derivative values of the torque and speed are used. Therefore, the estimation performance may be disappointing. In [20], a position control scheme was adopted so that the estimated results, which depend on position control performance, may be inaccurate.

This paper proposes a simple off-line identification integral algorithm, where the moment of inertia and friction constant are found. Since this is an off-line method, the main characteristics of the algorithm are similar to those described above. However, this method uses a pre-determined sinusoidal motion. As a result, the signals utilized for identification are less distorted. The parameters are identified using integral calculation, so that the algorithm is robust to noise whose mean is zero. Therefore, the results are relatively accurate.

II. Proposed Mechanical Parameter Identification Algorithm

This section describes the proposed mechanical parameter identification algorithm. The moment of inertia and the friction constant are identified using the torque reference of a speed controller and the speed of the mechanical system. Therefore, the algorithm is based on the mechanical system's speed control as shown in Fig. 1. Although Fig. 1 shows a block diagram with a rotational system, the algorithm can also be applied to a linear motion system. For convenience, the equations are described for rotational motion systems.

The mechanical system's dynamic equation can be described as below.

$$T_e = J_{eq}\dot{\omega} + B_{eq}\omega \tag{1}$$

where ω is the rotational speed of the motor and J_{eq} is the equivalent moment of inertia, which incorporates the motor and the mechanical system. B_{eq} is the equivalent viscous friction constant.

A. Estimation of Viscous Friction Constant

An equation to estimate the viscous friction constant can be described as follows. Both sides of (1) are multiplied by ω. Then a definite integral of (2) gives equation (3).

$$T_e\omega = J_{eq}\dot{\omega}\omega + B_{eq}\omega^2. \tag{2}$$

$$\begin{aligned}\int_{T_1}^{T_2} T_e(t)\cdot\omega(t)dt &= \frac{1}{2}J_{eq}\left(\omega^2(T_2)-\omega^2(T_1)\right)\\ &+ B_{eq}\int_{T_1}^{T_2}\omega^2(t)dt.\end{aligned} \tag{3}$$

If the speed at T_1 is equal to the speed at T_2, (3) can be simplified to (4), and the viscous friction constant can be estimated as equation (5). Therefore, the first condition for the estimation of the viscous friction constant is as described by (6).

$$\int_{T_1}^{T_2} T_e(t)\cdot\omega(t)dt = B_{eq}\int_{T_1}^{T_2}\omega^2(t)dt. \tag{4}$$

$$\hat{B}_{eq} = \frac{\int_{T_1}^{T_2} T_e(t)\cdot\omega(t)dt}{\int_{T_1}^{T_2}\omega^2(t)dt}. \tag{5}$$

$$\text{Condition I:}\quad \omega(T_1) = \omega(T_2). \tag{6}$$

The parameter estimation is performed using the torque command and speed feedback signals. Assuming that the speed control system is properly designed, the signals have no offset values. Only noises whose mean is zero are included in the signals.

As the integral interval increases, both of the integrals in (4) increase. If the integral interval is determined to be sufficiently long, the integral results in (4) become quite large and the influence of the noise on the integral calculation disappears. Therefore, the estimation accuracy increases.

B. Estimation of the Moment of Inertia

The moment of inertia can be expressed as follows. A definite integral of (1) gives (7). Then multiplication by ω gives (8), the definite integral of which is (9).

$$\int_{T_1}^{t} T_e(\tau)d\tau = J_{eq}(\omega(t)-\omega(T_1)) + B_{eq}(\theta(t)-\theta(T_1)). \tag{7}$$

$$\begin{aligned}\int_{T_1}^{t} T_e(\tau)d\tau\cdot\omega(t) &= J_{eq}(\omega^2(t)-\omega(T_1)\cdot\omega(t))\\ &+ B_{eq}\left(\theta(t)-\theta(T_1)\right)\cdot\omega(t).\end{aligned} \tag{8}$$

$$\begin{aligned}\int_{T_1}^{T_2}\left[\int_{T_1}^{t} T_e(\tau)d\tau\right]\cdot\omega(t)dt &= J_{eq}\int_{T_1}^{T_2}\omega^2(t)dt\\ &- J_{eq}\cdot\omega(T_1)\int_{T_1}^{T_2}\omega(t)dt\\ &+ B_{eq}\int_{T_1}^{T_2}\theta(t)\cdot\omega(t)dt - B_{eq}\cdot\theta(T_1)\int_{T_1}^{T_2}\omega(t)dt.\end{aligned} \tag{9}$$

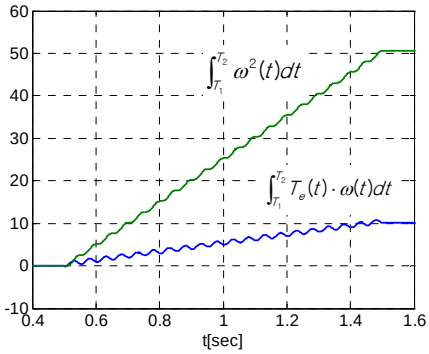

Fig. 2. Waveforms of the integral results from equation (5).

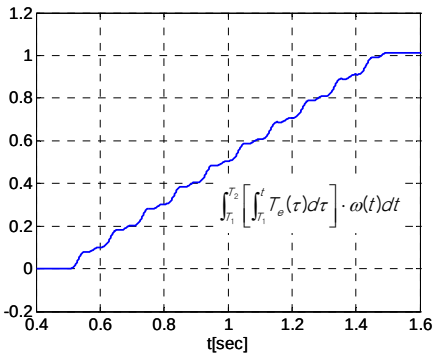

Fig. 3. Waveforms of the integral results from equation (12).

If the integral of the speed term, $\int_{T_1}^{T_2}\omega(t)dt$ is equal to zero, (9) is simplified to (10). In order for $\int_{T_1}^{T_2}\omega(t)dt$ to be zero, the speed must be periodic and have an average value of zero. Therefore, the integral interval should be a multiple of the speed reference period. Since the derivative of the angular position is the angular speed, $\int_{T_1}^{T_2}\theta(t)\cdot\omega(t)dt$ is also equal to zero. Therefore, (10) is simplified to (11) under Condition II. Finally, the equivalent moment of inertia can be estimated as (12).

$$\int_{T_1}^{T_2}\left[\int_{T_1}^{t}T_e(\tau)d\tau\right]\cdot\omega(t)dt = J_{eq}\int_{T_1}^{T_2}\omega^2(t)dt + B_{eq}\int_{T_1}^{T_2}\theta(t)\cdot\omega(t)dt. \tag{10}$$

$$\int_{T_1}^{T_2}\left[\int_{T_1}^{t}T_e(\tau)d\tau\right]\cdot\omega(t)dt = J_{eq}\int_{T_1}^{T_2}\omega^2(t)dt \quad \left(\because \int_{T_1}^{T_2}\theta(t)\cdot\omega(t)dt = 0\right). \tag{11}$$

$$\hat{J}_{eq} = \frac{\int_{T_1}^{T_2}\left[\int_{T_1}^{t}T_e(\tau)d\tau\right]\cdot\omega(t)dt}{\int_{T_1}^{T_2}\omega^2(t)dt}. \tag{12}$$

Condition II: $\int_{T_1}^{T_2}\omega(t)dt = 0.$ (13)

C. Speed Profile and Discussions

To satisfy Conditions I and II, the speed reference can be selected as a sinusoidal waveform with an average value of zero. For example, the speed reference profile, and the integral interval can be expressed as (14) and (15).

$$\omega^* = A\sin 2\pi f_{ID}t. \tag{14}$$

$$T_2 = T_1 + N\cdot T_{ID} \tag{15}$$

where A, f_{ID} and T_{ID} are the magnitude, frequency and period of the speed profile, respectively, and N is a positive integer.

The proposed method utilizes a sinusoidal speed profile to avoid rapid changes in the control variable. The derivative torque and speed values are not used in the estimation, which reduces distortion. Using a definite integral with a specific interval (T_1, T_2) together with equations (5) and (12), precise estimation results and robustness to measurement noise are obtained.

D. Simulations

Simulations of the proposed parameter identification were performed. In the simulations, the moment of inertia and the friction constant were set at 0.02 kg m^2 and 0.2 Nm s rad^{-1}, respectively. The speed reference magnitude was 100 r/min, and its frequency was 10 Hz. Therefore, the frequency and its multiples were included in the simulation waveforms. The estimation was performed over a period of 1 s from 0.5 s to 1.5 s. Therefore, the estimation was performed for ten periods of the speed reference.

Figs. 2 and 3 show the resulting waveforms of (5) and (12) respectively. $\int_{T_1}^{T_2}T_e(t)\cdot\omega(t)dt$ and $\int_{T_1}^{T_2}\omega^2(t)dt$ are shown in Fig. 2, and $\int_{T_1}^{T_2}\left[\int_{T_1}^{t}T_e(\tau)d\tau\right]\cdot\omega(t)dt$ is shown in Fig. 3. All of them are seen to increase with estimation time. Using these, the moment of inertia and friction constant are obtained.

Fig. 4 shows the estimation results, the friction constant, and the moment of inertia. Detailed waveforms are given in Fig. 5. The estimation results, B_{est} and J_{est}, oscillate during the estimation period, which can be increased to reduce oscillations. Additionally, at multiples of 0.1 s, B_{est} and J_{est} have the same value as the final simulation result. Therefore, for accurate data collection, the estimation interval should be a multiple of the period of the speed reference.

III. Implementation of the Proposed Algorithm

The proposed algorithm only needs the reference torque and the speed of the mechanical system, which can both be accessed in the control system. Assuming the speed is measured precisely, despite fluctuations, the estimation results should be accurate, as shown previously. Therefore, the proposed method should be useful for industrial applications.

Generally, position sensors such as encoders and resolvers

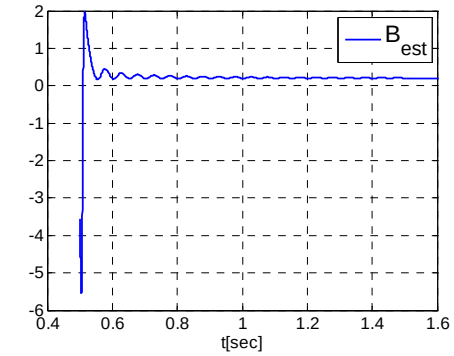

(a)

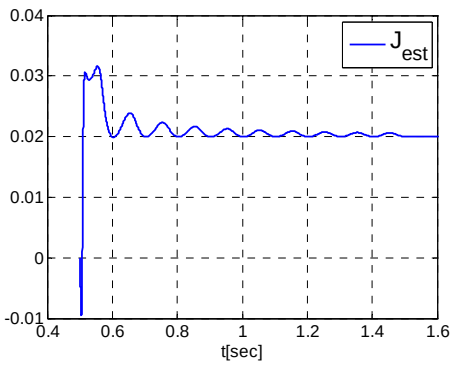

(b)

Fig. 4. Simulation results of the friction constant (a), and the moment of inertia (b).

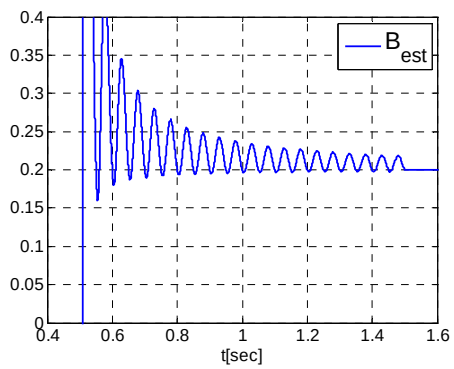

(a)

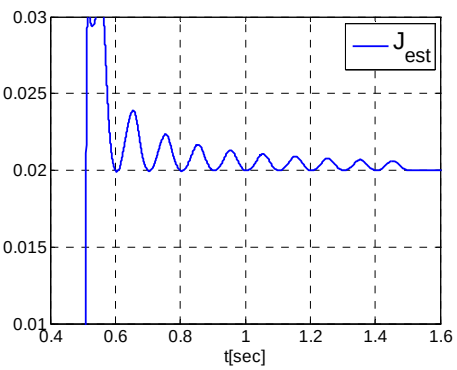

(b)

Fig. 5. Magnified waveforms of the simulation results of the friction constant (a), and the moment of inertia (b).

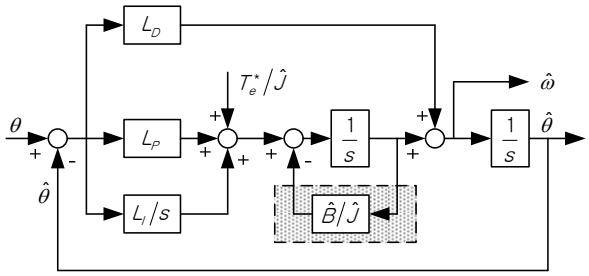

Fig. 6. Block diagram of a typical Luenberger observer.

are installed in mechanical systems. The position signal from a position sensor is not continuous. It has a discrete value and it can be modeled as the sum of the actual position and the quantization noise. Therefore, the derivative of the position signal increases the quantization noise. As a result, direct differentiation is not used in industry. Instead, to measure the speed of a mechanical system, the M/T method [23] and/or a Luenberger observer are adopted. If an encoder is installed, the M/T method can be utilized, and it shows reasonable performance in terms of speed estimation.

However, if a resolver is used to sense position instead of an encoder, the M/T method cannot be utilized for precise speed estimation. The estimated speed has more noise, especially at very low speeds including zero speed [24].

Alternatively, a Luenberger speed observer can be used, given its performance and well-understood theory. However, the performance depends on the accuracy of the system parameters, particularly the moment of inertia and the viscous friction coefficient. At a constant speed, the estimated speed is accurate. However, when the reference speed is sinusoidal the estimated speed shows some phase delay and magnitude errors according to the mechanical parameter errors. Any error in the estimated speed has a direct effect on the accuracy of any subsequent estimations.

In spite of this inaccuracy, a Luenberger observer can be adopted together with the proposed method. Errors in the mechanical parameters provided by the observer lead to errors in the identification of the mechanical parameters. However, these errors are gradually reduced. By repeating the identification several times, the identification results converge to the true parameters. Fig. 6 shows a typical implementation of a Luenberger observer. Assuming that the torque control performance of the servo system is ideal, the torque reference T_e^* is equal to the real torque. Therefore, the torque command can be described as (16). The transfer function of the estimated speed can be expressed as (17).

$$T_e^* = T_e = Js\omega + B\omega = Js^2\theta + Bs\theta. \tag{16}$$

$$\frac{\hat{\theta}}{\theta} = \frac{\hat{\omega}}{\omega} = \frac{\frac{J}{\hat{J}}s^3 + \left(\frac{B}{\hat{J}} + L_D\right)s^2 + \left(\frac{\hat{B}}{\hat{J}}L_D + L_P\right)s + L_I}{s^3 + \left(\frac{\hat{B}}{\hat{J}} + L_D\right)s^2 + \left(\frac{\hat{B}}{\hat{J}}L_D + L_P\right)s + L_I}. \tag{17}$$

TABLE I
SIMULATION RESULTS I

	$\hat{J}$	$\hat{B}$
Initial value	0.1000	2.0000
First trial	0.0183	0.1205
Second trial	0.0202	0.2210
Third trial	0.0200	0.1965
Fourth trial	0.0200	0.2005

TABLE II
SIMULATION RESULTS II

	$\hat{J}$	$\hat{B}$
Initial value	0.0050	2.0000
First trial	0.0227	-0.0008
Second trial	0.0195	0.2185
Third trial	0.0201	0.1990
Fourth trial	0.0200	0.1998

TABLE III
SIMULATION RESULTS III

	$\hat{J}$	$\hat{B}$
Initial value	0.1000	2.0000
First trial	0.0176	0.1550
Second trial	0.0202	0.2308
Third trial	0.0198	0.2330
Fourth trial	0.0198	0.2330

When the real moment of inertia, *J*, and the friction constant, *B*, are equal to their estimated values, $\hat{J}$ and $\hat{B}$, the transfer function is unity and the estimated speed is accurate. However, when the estimated mechanical parameters are inaccurate, the estimated speed is not equal to the real speed. Despite inaccurate speed information, by repeating the identification processes, the identification results can converge to the real value.

Tables I and II show the identification results when the process was performed four times. The real values of the moment of inertia and friction constant are 0.02, and 0.2, respectively. In Table I, the initial moment of inertia is 0.1, and the friction constant is 2 in the observer plant model. After the first trial, the identified results were used for the observer plant model in the second trial. After the second trial, the identified results were used in the third trial. Four iterations were performed, resulting in the accurate solutions seen in Table 1. In Table II, the initial moment of inertia was 0.005, and the friction constant was 2 in the observer plant model. The initial inertia value was smaller than the real value. After the first trial, the constant was estimated as -0.0008. Since negative values are impossible, zero was used for the observer in the second trial. Regardless of the initial values, the process performed well after four iterations.

A Luenberger observer is generally used to model only the inertia. This is done for the sake of simplicity. The friction torque loss, which is the shaded block in Fig. 6, is omitted. In this case, the transfer function can be addressed as per equation (18).

$$\frac{\hat{\theta}}{\theta}=\frac{\hat{\omega}}{\omega}=\frac{\frac{J}{\hat{J}}s^3+\left(\frac{B}{\hat{J}}+L_D\right)s^2+L_Ps+L_I}{s^3+L_Ds^2+L_Ps+L_I}. \quad (18)$$

As shown in (18), the transfer function cannot be unity, even if the estimated parameters are exact. Due to a small error in the estimated speed, the data cannot converge on the real value. Table III shows the results of the same algorithm as that shown in Table I, but with the torque losses due to friction omitted. The inertia result is somewhat accurate with an error of -1%. However, the friction constant error is as high as 16.5%. Therefore, to guarantee accuracy, the torque losses due to friction should be included in the observer plant model.

Generally, in high speed drive systems, Coulomb friction is quite small so that it can be neglected. However, in low speed drive systems such as conveyer belt systems and hoist systems, Coulomb friction is not negligible. Therefore, Coulomb friction should be considered for the accurate identification.

Mechanical system including Coulomb friction can be modeled as:

$$T_e=J_{eq}\dot{\omega}+B_{eq}\omega+C\cdot sign(\omega) \quad (19)$$

where *C* refers to Coulomb friction, which only depends on the direction of rotation. Therefore, Coulomb friction can be measured using constant-speed operations. In case of that the drive systems that operate in two positive speeds, ω_1 and ω_2, and the corresponding torque commands of the speed controller are $T_{e,1}$ and $T_{e,2}$, respectively. The Coulomb friction can be calculated as:

$$C=\frac{T_{e,1}\omega_2-T_{e,2}\omega_1}{\omega_2-\omega_1}. \quad (20)$$

Using the measured Coulomb friction, the mechanical system equation can be described as:

$$T_e'=T_e-C\cdot sign(\omega)=J_{eq}\dot{\omega}+B_{eq}\omega. \quad (21)$$

In order to avoid the effect of Coulomb friction, the parameter estimation given in (5) and (12) can be performed using T_e' instead of T_e.

IV. EXPERIMENTAL RESULTS

Experiments were performed with a motor to verify the effectiveness of the proposed method. The test setup consisted of a 5 kW surface-mounted permanent magnet synchronous machine (SMPMSM) and a 3.7 kW induction machine. They were directly coupled by a disc coupling. The proposed algorithm was implemented in the inverter for the SMPMSM. The induction machine did not operate. As a result, it served as an inertia load. The nominal parameters of the SMPMSM are listed in Table IV.

The proposed parameter estimation was performed. The

TABLE IV
NOMINAL PARAMETERS OF SMPMSM

Parameters	Values[unit]
Rated power	5.0 [kW]
Rated speed	3000 [r/min]
Number of pole	8
Rated voltage	200 [V_{RMS}]
Rated current	27.4 [A_{RMS}]
Stator resistance	0.05699 [Ω]
Stator inductance	0.55 [mH]

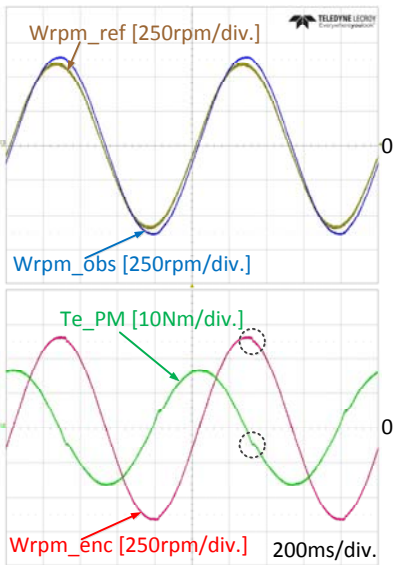

Fig. 7. Speed and torque waveforms for parameter identification

motor to which the algorithm was applied was speed-controlled with a sinusoidal speed reference. The magnitude and frequency of the speed reference were 600 r/min and 1 Hz, respectively. Fig. 7 shows the speed-controlled performance. The speed reference, the speed estimated by the Luenberger observer, the speed estimated by the M/T method, and the output torque of the SMPMSM are shown in Fig. 7. A simple PI controller was used as a speed regulator. Therefore, the magnitude of the real speed was slightly larger than that of the speed reference, and the real speed lagged behind the reference.

The motors were directly disc coupled (a single flexible coupling). Due to flexibility, there were small torque distortions in the waveforms when the polarity of the output torque was switched from positive to negative, and vice versa. The distortion is highlighted with the dashed circle in Fig. 7. At that time, the speed waveform estimated by the M/T method also had a small step variation for the same reason.

To reduce the influence of distortions on parameter estimation, the frequency of the speed reference should be smaller than a certain threshold. As the frequency increases, the distortion from the disc flexibility increases in severity, and the estimation error is increased. The output torque is reduced as the frequency decreases. Here, the required calculation time is increased due to limited torque

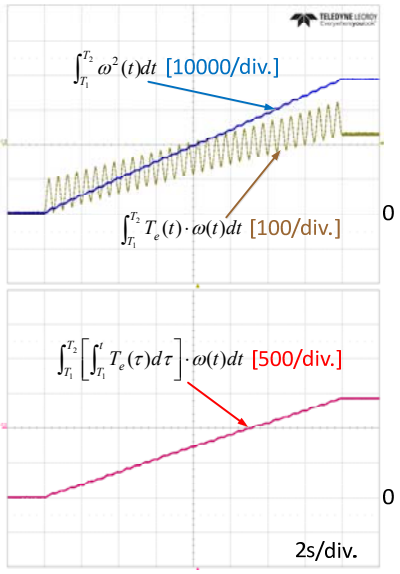

Fig. 8. Waveforms of the integral calculations.

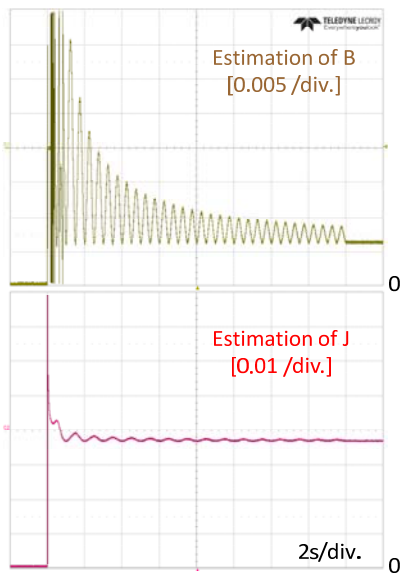

Fig. 9. Waveforms of the estiated mechanical paraeters.

information. As a result, in the experiment, the frequencies for identification were selected to be 1, 0.75, and 0.5 Hz. Experimental waveforms at 1 Hz are displayed in Figs. 7, 8 and 9.

The mechanical parameters were estimated from the torque and the speed. Fig. 8 shows the integral calculation results for mechanical parameter identification, which took 16 s. The waveforms in Fig. 8 show $\int_{T_1}^{T_2}\omega^2(t)dt$, $\int_{T_1}^{T_2}T_e(t)\cdot\omega(t)dt$, and $\int_{T_1}^{T_2}\left[\int_{T_1}^{t}T_e(\tau)d\tau\right]\cdot\omega(t)dt$, which increase as the estimation time increases. The waveforms have fluctuations of 2 Hz, due to the frequency of the speed reference (1 Hz).

From these values, the moment of inertia and the friction constant are estimated. Fig. 9 shows the estimated results.

TABLE V
RESULTS OF THE M/T METHOD

		$\hat{J}$	$\hat{B}$
1 Hz	First estimation	0.03670	0.005984
	Second estimation	0.03672	0.005963
0.75 Hz	First estimation	0.03670	0.006755
	Second estimation	0.03669	0.006714
0.5 Hz	First estimation	0.03664	0.007261
	Second estimation	0.03664	0.007252

TABLE VI
RESULTS OF AN OBSERVER WITH A 1 HZ SPEED REFERENCE

	$\hat{J}$	$\hat{B}$
Initial value	0.3	0.1
First trial	0.03585	0.005761
Second trial	0.03677	0.007703
Third trial	0.03674	0.007534
Fourth trial	0.03673	0.007535

TABLE VII
RESULTS OF AN OBSERVER WITH A 0.75 HZ SPEED REFERENCE

	$\hat{J}$	$\hat{B}$
Initial value	0.3	0.1
First trial	0.03608	0.006881
Second trial	0.03667	0.007665
Third trial	0.03666	0.007616
Fourth trial	0.03664	0.007622

TABLE VIII
RESULTS OF AN OBSERVER WITH A 0.5 HZ SPEED REFERENCE

	$\hat{J}$	$\hat{B}$
Initial value	0.3	0.1
First trial	0.03628	0.007512
Second trial	0.03662	0.007700
Third trial	0.03663	0.007685
Fourth trial	0.03663	0.007692

The mechanical parameters are calculated as equations (5) and (12), with results similar to those of the simulations. As the estimation period increased, the oscillations became smaller. At time points in multiples of 1 s, the period of the speed reference, the identified mechanical parameters were the same as the final results. Therefore, the identification interval should be an integer multiple of the period of the speed reference for accurate data acquisition.

Table V shows identification results based on the speed from the M/T method. Using speed references of 1, 0.75, and 0.5 Hz, the proposed estimation was performed. As shown in Table V, the identified moments of inertia were similar across the frequency range. There was an error between them of less than 1%. It can be concluded that the estimation accuracy of this proposed method is remarkably good.

The results of the viscous friction coefficient varied slightly between the frequencies. This may have resulted from un-modelled factors, such as windage loss, stray loss

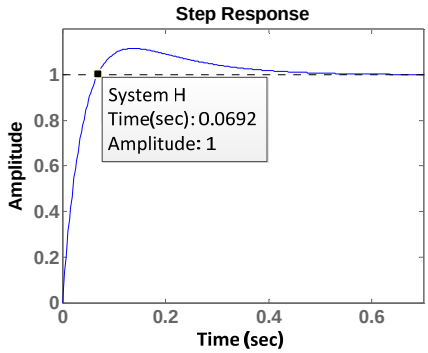

Fig. 10. Step response of the speed regulator.

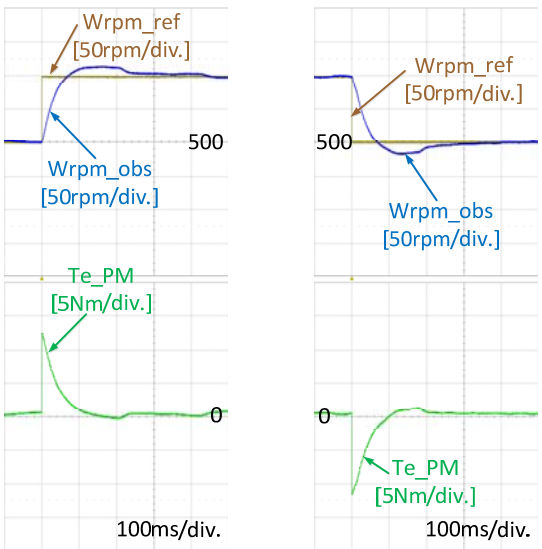

Fig. 11. Experimental step response of the speed regulator from 500 to 600 r/min (a), and vice versa (b).

etc., which may affect the friction coefficient. The error in the friction coefficient are reduced if the viscous friction term is larger than the un-modelled factors.

Tables VI, VII, and VIII show identification results based on the speed from the Luenberger observer shown in Fig. 6. Assuming that the mechanical properties were unknown, the initial values for the observer were selected to be relatively large, considering the power rating of the mechanical systems. After four iterations, the algorithm converged on a set of solutions with an error of less than 1% between them. The results are similar to those obtained with the M/T method.

To verify the accuracy of the results, a PI speed controller was designed with the measured moment of inertia. The transfer function of the speed regulation can be expressed as:

$$\frac{\omega}{\omega^*} = \frac{2\varsigma\omega_n s + \omega_n^2}{s^2 + 2\varsigma\omega_n s + \omega_n^2} \tag{19}$$

where ω_n is $2\pi \cdot 5$, and ς is $\sqrt{5}/2$, which results in a slightly over-damped system. Fig. 10 shows the step response of the designed speed regulator. Fig. 11 shows the step response from the experimental data. The speed reference was changed

from 500 to 600 r/min and vice versa. Comparing the figures, the performance of the speed regulator coincides well with the designed response. Based on the experimental results, it can be concluded that the proposed estimation method is accurate.

V. CONCLUSIONS

This paper presents a method for the identification of mechanical parameters, based on integral calculation, which is robust against measurement noise. Using excitation conditions that avoid distortion, the accuracy of the parameter identification is improved. The identified moment of inertia and friction constant are utilized for the design of speed and position controllers, and various kinds of observers. As a result, the control performance of mechanical systems can be enhanced. Due to the simplicity of the proposed method, this approach can easily be applied to commercial inverter products with no additional expense.

ACKNOWLEDGMENT

This work was supported by the Basic Science Research Program (NRF - 2014R1A1A1005138) through the NRF of Korea funded by the MSIP(Ministry of Science, ICT & Future Planning) of Korea, and the New & Renewable Energy Core Technology Program (No. 20143030071320) of the KETEP, granted financial resource from the MOTIE (Ministry of Trade, Industry & Energy) of Korea.

REFERENCES

[1] S. K. Kuo and C. H. Menq, "Modeling and control of a six-axis precision motion control stage," *IEEE/ASME Trans. Mechatronics*, Vol. 10, No. 1, pp. 50–59, Feb. 2005.

[2] J. H. Kim, J. W. Choi, and S. K. Sul, " High precision position control of linear permanent magnet synchronous motor for surface mount device placement system," *Conf. Rec. of PCC*, pp. 37-42, 2002.

[3] D. Li-Jun, S. Da-nan, D. Kan, Z. Lei-Ting, and L. Zhi-Gang, "Optimized design of discrete traction induction motor model at low-switching frequency," *IEEE Trans. Power Electron.*, Vol. 28, No. 10, pp. 4803-4810, Oct. 2013.

[4] S. Ziaeinejad, Y. Sangsefidi, H. P. Nabi, and A. Shoulaie, "Direct torque control of two-phase induction and synchronous motors," *IEEE Trans. Power Electron.*, Vol. 28, No. 8, pp. 4041-4050, Aug. 2013.

[5] S. K. Sahoo, S. Dasgupta, S. K. Panda, and J. X. Xu, "A lyapunov function-based robust direct torque controller for a switched reluctance motor drive system," *IEEE Trans. Power Electron.*, Vol. 27, No. 2, pp. 555-564, Feb. 2012.

[6] M. Pacas and J. Weber, "Predictive direct torque control for the PM synchronous machine," *IEEE Trans. Ind. Electron.*, Vol. 52, No. 5, pp. 1350-1356, Oct. 2005.

[7] H. Jiabing and Z. Q. Zhu, "Improved voltage-vector sequences on deadbeat predictive direct power control of reversible three-phase grid-connected voltage-source converters," *IEEE Trans. Power Electron.,* Vol. 28, No. 1, pp. 254-267, Jan. 2013.

[8] J. C. Moreno, J. M. E. Huerta, R. G. Gil, and S. A. Gonzalez, "A robust predictive current control for three-phase grid-connected inverters," *IEEE Trans. Ind. Electron.*, Vol. 56, No. 6, pp. 1993-2004, Jun. 2009.

[9] H. B. Shin and J. G. Park, "Anti-windup PID controller with integral state predictor for variable-speed motor drives," *IEEE Trans. Ind. Electron*., Vol. 59, No. 3, pp. 1509-1516, Mar. 2012.

[10] W. S. Huang, C. W. Liu, P. L. Hsu, and S. S. Yeh, "Precision control and compensation of servomotors and machine tools via the disturbance observer," *IEEE Trans. Ind. Electron.*, Vol. 57, No. 1, pp. 420-429, Jan. 2010.

[11] T. J. Kweon and D. S. Hyun, "High-performance speed control of electric machine using low-precision shaft encoder," *IEEE Trans. Power Electron.*, Vol. 14, No. 5, pp. 838-849, Sep. 1999.

[12] H. Kobayashi, S. Katsura, and K. Ohnishi, "An analysis of parameter variations of disturbance observer for motion control," *IEEE Trans. Ind. Electron.*, Vol. 54, No. 6, pp. 3413-3421, Dec. 2007.

[13] J. Yao, Z. Jiao, and D. Ma, "Adaptive robust control of DC motors with extended state observer," *IEEE Trans. Ind. Electron.*, Vol. 61, No. 7, pp. 3630-3637, Jul. 2014.

[14] J. W. Choi, S. C. Lee, and H. G. Kim, "Inertia identification algorithm for high-performance speed control of electric motors," *IEE Proc.— Electr. Power Appl.*, Vol. 153, No. 3, pp. 379-386, 2006.

[15] K. B. Lee, J. Y. Yoo, J. H. Song, and I. Choy, "Improvement of low speed operation of electric machine with an inertia identification using ROELO," *IEE Proc.— Electr. Power Appl.*, Vol. 151, No. 1, pp. 116-120, Jan. 2004.

[16] A. K. Sanyal, M. Chellappa, J. L. Valk, J. Ahmed, J. Shen, and D. S. Bernstein, "Globally convergent adaptive tracking of spacecraft angular velocity with inertia identification and adaptive linearization," in *Proc. 42nd IEEE Int. Conf. Decision Control*, Vol. 3, pp. 2704-2709, 2003.

[17] Y. Guo, L. Huang, and M. Muramatsu, "Research on inertia identification and auto-tuning of speed controller for AC servo system," *in Proc. Power Conversion Conf.*, Vol. 2, pp. 896-901, 2002.

[18] N. Li, X. Dianguo, Y. Ming, G. Xianguo, and L. Zijian, "On-line inertia identification algorithm for PI parameters optimization in speed loop," *IEEE Trans. Power Electron.*, Vol. 30, No. 2, pp. 849-859, Feb. 2015.

[19] T. S. Kwon, S. K. Sul, H. Nakamura, and K. Tsuruta, "Identification of the mechanical paramteres for servo drive," *Conf. Rec. of IAS Annual Meeting*, pp. 905-910, 2006.

[20] F. Andoh, "Moment of inertia identification using the time average of the product of torque reference input and motor position," *IEEE Trans. Power Electron.*, Vol. 22, No. 6, pp. 2534-2542, Nov. 2007.

[21] F. Andoh, "Inertia identification method based on the product of the integral of torque reference input and motor speed," in *Proc. IEEE Int. Conf. Control Appl.*, pp. 1151-1158, 2008.

[22] R. Garrido and A. Concha, "Inertia and friction estimation of a velocity-controlled servo using position measurements," *IEEE Trans. Ind. Electron.*, Vol. 61, No. 9, pp. 4759-4770, Sep. 2014.

[23] T. Ohmae, T. Matsuda, K. Kamiyama and M. Tachikawa, "A microprocessor-controlled high-accuracy wide-range speed regulator for motor drives," *IEEE Trans. Ind. Electron.*, Vol. 29, No. 3, pp. 207-211, Aug. 1982.

[24] H. W. Kim and S. K. Sul, "A new motor speed estimator using Kalman filter in low-speed range," *IEEE Trans. Ind. Electron.*, Vol. 43, No. 4, pp. 498-504, Aug. 1996.

Sang-Heon Han was born in Korea, in 1991. He received his B.S. degree in Electrical Engineering from Myongji University, Yongin, Korea, in 2009, where he has been working towards his M.S. degree since 2015. His current research interests include power electronic control of electric machines, sensorless drives, and power conversion circuits.

Anno Yoo received his B.S., M.S., and Ph.D. degrees in Electrical Engineering from Seoul National University, Seoul, Korea, in 2004, 2006, and 2010, respectively. From 2010 to 2015, he was a Senior Research Engineer with LSIS Co., Ltd., Anyang, Korea. From 2015 to 2016, he was a Senior Research Engineer with Mando Corporation, Seongnam, Korea. Since 2016, he has been a Senior Motor Controls Engineer with General Motors, Pontiac, MI, USA. His current research interests include high performance electric machine drives, electric machine modeling, and power conversion systems for electric/hybrid vehicles. He is holder of 6 registered patent in the United States and was a recipient of a 2015 Best Paper Award from the Journal of Power Electronics (2nd Prize).

Sang Won Yoon received his B.S. degree in Electrical Engineering from Seoul National University, Seoul, Korea, in 2000; and his M.S. and Ph.D. degrees in Electrical Engineering and Computer Science from the University of Michigan, Ann Arbor, MI, USA, in 2003 and 2009, respectively. From 2009 to 2013, he was Senior Scientist and Staff Researcher at the Toyota Research Institute of North America, Ann Arbor, MI, USA, where he conducted research in the fields of power electronics and sensor systems for automobiles. Since 2013, he has been with the Department of Automotive Engineering, Hanyang University, Seoul, Korea, where he is presently working an Assistant Professor. His current research interests include power electronics, sensors and sensor systems, electronic reliability, micro-/nanotechnology, and their applications in both conventional and future vehicles.

Young-Doo Yoon was born in Korea. He received his B.S., M.S., and Ph.D. degrees in Electrical Engineering from Seoul National University, Seoul, Korea, in 2002, 2005, and 2010, respectively. From 2010 to 2013, he was a Senior Engineer with Samsung Electronics Company, Korea. Since 2013, he has been an Assistant Professor in the Department of Electrical Engineering, Myongji University, Yongin, Korea. His current research interests include power-electronic control of electric machines, high power converters, and electric home appliances.